arXiv:patt-sol/9610009v1 23 Oct 1996

KUNS-1411
HE(TH) 96/12
Niigata 96/E1
Aichi-5/96
patt-sol/9610009

Solvable Optimal Velocity Models and Asymptotic Trajectory

Ken Nakanishi[*]
Department of Physics, Kyoto University, Kyoto 606-01, Japan

Katsumi Itoh[†] Yuji Igarashi[‡]
Physics Division, Dept. of Education, Niigata University, Niigata 950-21, Japan

Masako Bando[§]
Physics Division, Aichi University, Miyoshi, Aichi 470-02, Japan

October 23, 1996

Abstract

In the Optimal Velocity Model proposed as a new version of Car Following Model, it has been found that a congested flow is generated spontaneously from a homogeneous flow for a certain range of the traffic density. A well-established congested flow obtained in a numerical simulation shows a remarkable repetitive property such that the velocity of a vehicle evolves exactly in the same way as that of its preceding one except a time delay T. This leads to a global pattern formation in time development of vehicles' motion, and gives rise to a closed trajectory on Δx-v (headway-velocity) plane connecting congested and free flow points. To obtain the closed trajectory analytically, we propose a new approach to the pattern formation, which makes it possible to reduce the coupled car following equations to a single difference-differential equation (Rondo equation). To demonstrate our approach, we employ a class of linear models which are exactly solvable. We also introduce the concept of "asymptotic trajectory" to determine T and v_B (the backward velocity of the pattern), the global parameters associated with vehicles' collective motion in a congested flow, in terms of parameters such as the sensitivity a, which appeared in the original coupled equations.

---

[*] e-mail address: nakanisi@gauge.scphys.kyoto-u.ac.jp
[†] e-mail address: itoh@ed.niigata-u.ac.jp
[‡] e-mail address: igarashi@ed.niigata-u.ac.jp
[§] e-mail address: bando@aichi-u.ac.jp

1 Introduction

Traffic flow is one of the most interesting phenomena of many-body systems which may be controlled by basic dynamical equation. Recent developments in study of traffic flow has brought a renewed interest in microscopic approaches, such as Optimal Velocity Model (OV-model) [1, 2, 3], which is a new version of Car Following Model [4, 5, 6], Cellular Automaton Models [7, 8, 9], Coupled Map Lattice Models [10] and Fluid Dynamical Models [11]. The OV-model, among others, has especially attracted interest because it provides us with a possibility of unified understanding of both free and congested traffic flows from common basic dynamical equations. Unlike traditional Car Following models, it introduces Optimal Velocity Function $V(\Delta x)$ as a desirable velocity depending on headway distance Δx. The basic equation of OV-model for a series of vehicles on a circuit of length L is,

$$\ddot{x}_n(t) = a\{V(\Delta x_n(t)) - \dot{x}_n(t)\} \qquad n = 1, 2 \cdots N, \tag{1}$$

where x_n denotes the position of the n-th vehicle, $\Delta x_n \equiv x_{n-1} - x_n$ headway and N the total vehicle number. The constant parameter a is the sensitivity. A driver accelerates (or decelerates) his vehicle in proportion to the difference between his velocity and the optimal velocity $V(\Delta x)$. As easily noticed, a homogeneous flow is a solution to Eq. (1). In such a flow, vehicles have a common headway L/N, which is the inverse of the vehicle density. Stability of homogeneous flows is analyzed within a linear approximation[1, 2]; it is stable for $f = V'(L/N) < f_c$ and unstable for $f > f_c$. The critical value is found to be $f_c = a/2$.

In order to demonstrate that the OV-model describes “spontaneous generation of congestion”, numerical simulations were made using Eq. (1). It was found that for $f < f_c$, i.e., if the density is above the critical value, a slightly perturbed homogeneous flow develops to a congested flow after enough time. The congested flow consists of alternating two distinct regions; congested regions (high density), and smoothly moving regions or free regions (low density). In this way the traffic congestion occurs spontaneously in the OV-model. This phenomenon can be understood as a sort of phase transition from a homogeneous flow state to a congested flow state [1, 2].

A remarkable feature of the well-established congested flow is that the velocity of the n-th vehicle $\dot{x}_n$ has the same time dependence as that of the preceding ($(n-1)$-th) vehicle except a certain time delay T. It is also found that the global pattern moves backward with a velocity v_B. This kind of behavior of vehicles may be called “repetitive pattern formation”. It leads to formation of a closed trajectory (“limit cycle”) on Δx-v plane, along which representative points for all the vehicles move one after another. The convergence of vehicles’ trajectories to a closed trajectory signals the congestion in a traffic flow. Therefore the determination of the closed trajectory is one of the most important subjects to understand congested flows. However this has been done mostly in computer simulations. The purpose of the present paper is to obtain this closed trajectory directly by an analytical method. Actually it has been found that, in the vicinity of the critical point for the congested flow, equation (1) can be reduced to the modified KdV equation by the dynamical reduction method [12]. In this paper we propose a new analytical approach to the pattern formation, which may be applicable to any congested flow.

We argue that, once the repetitive pattern is formed, the coupled car following equations reduce to a single difference-differential equation (Rondo equation) for a universal function (Rondo function). A Rondo function determines a closed trajectory on Δx-v plane. To make the Rondo equation tractable, we have simplified our question on the following two points: firstly we have assumed that OV-functions are piece-wise linear; secondly we have concentrated our attention to an asymptotic trajectory, which is the key concept to be explained in the next section. We would like to stress that our method does not lose its generality by making the above assumption on OV-functions: an OV-function to be obtained from real data may be approximated by a piece-wise linear function.

With the above simplifications, we have solved the Rondo equation for each model and given an asymptotic trajectory on the Δx-v plane. Our result clearly tells us that, once an OV-function and the sensitivity a are given, an asymptotic trajectory is uniquely determined; this then implies that the parameters T and v_B for a collective motion of vehicles are given as a function of a. Therefore our approach provides us with a method to determine a dependence of the global parameters T and v_B.

This paper is organized as follows. Next section summarizes the main results obtained from numerical simulations of the OV-model, with emphasis on the pattern formation in a congested flow. The concept of an asymptotic trajectory is explained in this section. As will become clear in later sections, an asymptotic trajectory is a very important concept to understand the OV-model. We derive the difference-differential equation and present a general strategy on how to solve it in section 3. This part summarizes the central idea of this paper. In order to demonstrate how the Rondo approach works, we analytically solve, in section 4, some simple models with piece-wise linear OV-functions. Our first model has been investigated by Sugiyama and Yamada[13]. Here we solve this model in the context of the Rondo approach. Although an asymptotic trajectory is very close to a real trajectory observed in a computer simulation, it is not exactly the same to the latter. We describe some aspects of real trajectories based on our knowledge of the asymptotic one in section 5. The final section is devoted to summary and discussions.

2 Pattern Formation in OV-Model

Let us recollect what we have learned with numerical simulations of an OV-model [1, 2, 3]. Suppose a simulation is performed with a given OV-function and a fixed sensitivity a. After a congested flow is well-established, typical features of the repetitive behavior can be observed in the following two figures.

Figs. 1(a) and (b) show that vehicles move in alternating regions of free and congested flows. It is recognized that every vehicle behaves in the same manner as its preceding one with a certain time delay T: as a result, the congested region moves backward with the velocity v_B. Once the location of any vehicle, say, the n-th vehicle, is given as a function of t, we may reproduce the pattern in Fig. 1(a) by plotting a series of functions shifted in time and position by T and $v_B T$ appropriately. Therefore we expect that a congested flow may be completely determined by a function of t and global parameters T and $v_B T$. The precise specifications of our approach to this repetitive behavior will be explained in the next section.

Fig. 1(b) clearly shows there exists a “limit cycle” on the Δx-v plane, a closed curve with two cusps at points C $(\Delta x_{\mathrm{C}}, v_{\mathrm{C}})$ and F $(\Delta x_{\mathrm{F}}, v_{\mathrm{F}})$, both of which are on the OV-function. At these cusp points, we find $V'(\Delta x) < a/2$, which means that homogeneous flows with such headways and velocities are linearly stable. Representative points for all

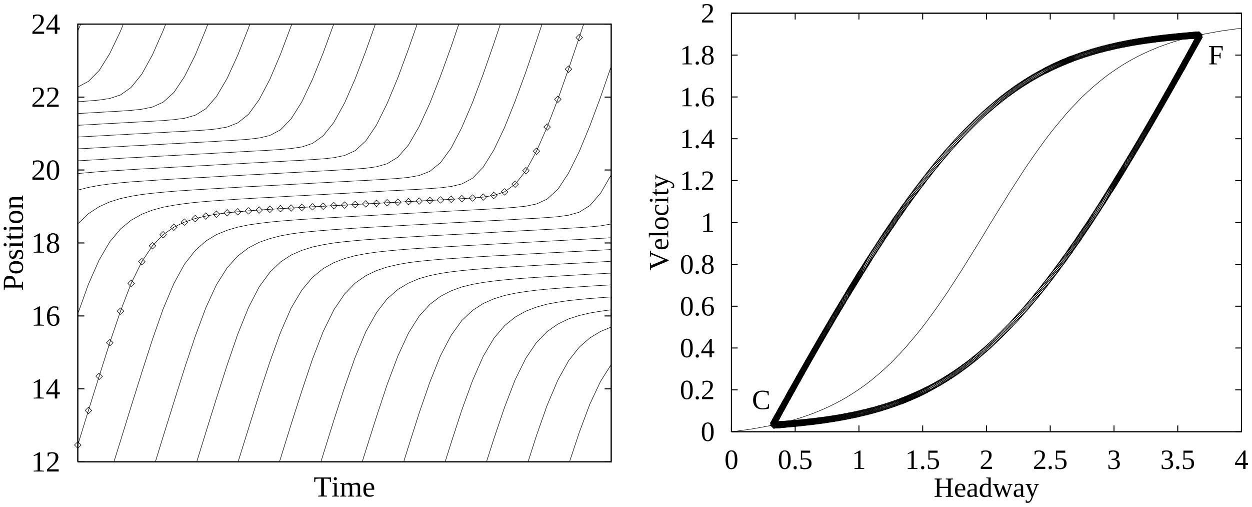

Figure 1: A result of the numerical simulation with 20 vehicles on a circuit with the circumference $L = 40$. The sensitivity and the OV-function are chosen as $a = 1.0$ and $V(h) = \tanh(h-2) + \tanh(2)$. (a) Trajectories of vehicles passing through a congested region. (b) The "limit cycle" on the Δx-v (headway-velocity) plane. The cusp points C and F correspond to congested and free regions respectively. Representative points for vehicles move anti-clockwise along this "limit cycle". They run fast on curves connecting the two cusps, while they stay around cusps for a while. The thin line shows the OV-function.

vehicles move on this "limit cycle" in the same direction as anti-clockwise. It follows from the conservation of flow,

$$\frac{v_{\rm C} + v_B}{\Delta x_{\rm C}} = \frac{v_{\rm F} + v_B}{\Delta x_{\rm F}} = \frac{1}{T}, \tag{2}$$

that the straight line connecting C and F has the slope T^{-1} and intersects with the vertical axis at $-v_B$.[1]

In the rest of this section, we would like to explain the concept of an asymptotic trajectory on the Δx-v plane. Suppose that a vehicle passes through two congested regions different in size on a circuit. Then the representative point moves on curves as shown in Fig. 2. Each trajectory may not form an actual cusp, rather it will form a round shaped tip. Also we find that the larger the congested region, the sharper the shape of the tip: the minimum velocity of the vehicle is smaller for a longer congestion. It is rather easy to imagine that for a very short congestion the vehicle cannot decelerate itself enough to reach the velocity appropriate for a longer congested region. If we plot minimum velocities for longer and longer congested regions, we would find a limiting value for the minimum velocities. This value must be realized for an infinitely long congested region. With a similar argument we find the limiting value for maximum velocities corresponding to an infinitely long free region. We may imagine the following extreme situation: a vehicle starting from an infinitely long free (congested) region goes toward an infinitely long congested (free) region. The trajectory for this limiting situation will be called as a decelerating (an accelerating) asymptotic trajectory. Combining them we would find a closed curve with two real cusps on the OV-function.

---

[1] This relation is an approximate one except for an asymptotic trajectory to be discussed below.

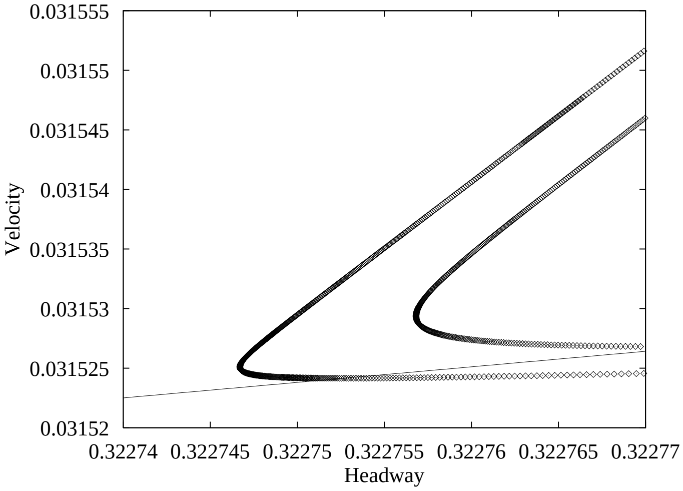

Figure 2: Trajectories for a vehicle passing through two congested regions different in size. The outer curve corresponds to the larger congested region. The thin line is the OV-function. Parameters are the same as those in Figure 1.

The duration for a vehicle to stay in a congested region would obviously get longer for a larger congested region. For an asymptotic trajectory it becomes infinite. This does fit to our linear analysis since the behavior of a vehicle is controlled by exponential functions in time. In section 5, we shall see that exponential functions determine a curve near a cusp.

3 Rondo Approach

We begin our description of the Rondo approach with two basic assumptions:

1. Velocities of the n-th and $(n-1)$-th vehicles have exactly the same time dependence if a certain time delay T is taken into account, $\dot{x}_{n-1}(t) = \dot{x}_n(t+T)$.
2. The pattern of traffic flow moves backward with a constant velocity v_B.

The above described properties are expressed as,

$$x_{n-1}(t) = x_n(t+T) + v_B T. \tag{3}$$

All the vehicles' behavior is represented with a single universal function $F(t) \equiv x_n(t)$;[2]

$$x_{n-k}(t) = F(t+kT) + k v_B T. \tag{4}$$

With n-th vehicle's headway given as

$$\Delta x_n(t) = F(t+T) - F(t) + v_B T, \tag{5}$$

N coupled car following equations (1) are reduced to a single difference-differential equation for $F(t)$,

$$\frac{1}{a}\ddot{F}(t) + \dot{F}(t) = V(F(t+T) - F(t) + v_B T). \tag{6}$$

---

[2] This assumption bares some similarities with the travelling wave ansatz ($\phi(x,t) \to f(x-vt)$) for the wave equation.

In the following it will be called the Rondo equation.

In this paper, we will seek the Rondo function $F(t)$ for the asymptotic trajectory.[3] Before studying concrete models, let us consider its generic properties. Since the position and the velocity of vehicles are obviously continuous in time, $F(t)$ is a continuously differentiable function.

An asymptotic trajectory connects the points F and C, each of which corresponds to an infinitely long free or congested region (an approximately homogeneous flow) satisfying the stability condition mentioned in section 2. Therefore $F(t)$ should be homogeneous flows asymptotically in the infinite past and future: $\dot{F}(t) \to$ const. as $t \to \pm\infty$. An asymptotic trajectory interpolates two stable solutions of the equation (1). In this sense $F(t)$ may be regarded as a "kink solution".

Like OV-models studied in earlier papers, each model in the next section has an OV-function which is symmetric with respect to a point, $\mathrm{S}(\Delta x_{\mathrm{S}}, v_{\mathrm{S}})$.[4] So we assume this property in the following arguments and quote our result in appendix A. Two end points of an asymptotic trajectory, $\mathrm{C}(\Delta x_{\mathrm{C}}, v_{\mathrm{C}})$ and $\mathrm{F}(\Delta x_{\mathrm{F}}, v_{\mathrm{F}})$, are symmetric with respect to S. Three points C, F and S are on a straight line with a slope T^{-1} and an intersection $-v_B$. Note that once the slope is given, the intersection is uniquely determined since the point S must be on the line.

As shown in appendix A, accelerating and decelerating asymptotic trajectories are symmetric with respect to S. Therefore it is sufficient to study one of them; in the rest of this paper, we will take an decelerating asymptotic trajectory. Here we summarize conditions which should be satisfied by the function $F(t)$:

1) $F(t)$ and $\dot{F}(t)$ are continuous for any t ($F(t) \in C^1$);

2) $v_{\mathrm{F}} = \lim_{t\to-\infty} \dot{F}(t)$ and $v_{\mathrm{C}} = \lim_{t\to+\infty} \dot{F}(t)$;

3) $v_{\mathrm{F}} + v_{\mathrm{C}} = 2v_{\mathrm{S}}$ and $\Delta x_{\mathrm{F}} + \Delta x_{\mathrm{C}} = 2\Delta x_{\mathrm{S}}$, where $\Delta x_{\mathrm{F}} = \lim_{t\to-\infty}(F(t+T) - F(t) + v_B T)$ and $\Delta x_{\mathrm{C}} = \lim_{t\to+\infty}(F(t+T) - F(t) + v_B T)$.

We would like to explain a way to solve the Rondo equation, which contains an OV-function and a sensitivity a as well as T and v_B associated the pattern formation. (1) First we give the parameter T. By drawing a straight line through the point S with the slope T^{-1}, we find the intersection $-v_B$ and the points C and F. (2) Now a is the only free parameter of the Rondo equation. If we could solve the equation, we would obtain a one-parameter family of (or a-dependent) Rondo functions. (3) Among this family, the right Rondo function is selected by requiring that it connects the points C and F. This condition also determines a unique value for a. Accordingly we find the a-dependence of T.

4 Piece-wise Linear Function Models

We consider here a class of models with piece-wise linear OV-functions. The Rondo equation is now linearized for all regions of Δx, and therefore exactly solvable.

---

[3] We will discuss more realistic situations with finite congested regions in section 5.

[4] The symmetry of an OV-function is absolutely not necessary to solve a system in the Rondo approach. In the last section, we discuss how to solve the Rondo equation for a generic situation.

4.1 Step Function Model

The first model has the step function for the OV-function,

$$V(\Delta x) = \begin{cases} 0 & \Delta x < \Delta x_{\mathrm{S}} \quad \text{(region I)} \\ V_0 & \Delta x > \Delta x_{\mathrm{S}} \quad \text{(region II).} \end{cases} \tag{7}$$

This OV-model has been solved in Ref. [13]. Here we explain how this model can be solved in our Rondo approach. In this model, the Rondo equation is given by

$$\frac{1}{a}\ddot{F}(t) + \dot{F}(t) = V_0\, \theta\left(F(t+T) - F(t) + v_B T - \Delta x_{\mathrm{S}}\right), \tag{8}$$

where $\theta(x)$ is the Heviside function.

In the motion corresponding to a decelerating asymptotic trajectory, the representative point for a vehicle moves from region II into region I. Let us take the time t such that the point moves into the region I at $t = 0$, which implies $\Delta x_n(0) = \Delta x_{\mathrm{S}}$.

The equation of motion is

$$\frac{1}{a}\ddot{F}(t) + \dot{F}(t) = \begin{cases} V_0 & (t < 0) \\ 0 & (t > 0). \end{cases} \tag{9}$$

The general solutions for two regions are

$$\dot{F}(t) = \begin{cases} V_0 + C_1 e^{-at} & (t \le 0) \\ C_2 e^{-at} & (t \ge 0). \end{cases} \tag{10}$$

The integration constants are determined as $C_1 = 0$ and $C_2 = V_0$ from requirements that $\dot{F}(t)$ be a continuous function and asymptotically constant for $t \to \pm\infty$. The continuous function $F(t)$ is

$$F(t) = \begin{cases} V_0 t & (t \le 0) \\ \dfrac{V_0}{a}(1 - e^{-at}) & (t \ge 0). \end{cases} \tag{11}$$

Here we choose the origin of position coordinate so that $F(0) = 0$.

The function $F(t)$ with its relation to the headway, $\Delta x_n(t) = F(t+T) - F(t) + v_B T$, completely determines a decelerating asymptotic trajectory on the Δx-v plane. From the condition 3) in the section 3, the asymptotic trajectory connects symmetric points on the OV-function. This gives us a condition $\Delta x_n(+\infty) + \Delta x_n(-\infty) = 2\Delta x_{\mathrm{S}} = 2\Delta x_n(0)$,

$$v_B T + (V_0 + v_B)T = 2\left[\frac{V_0}{a}(1 - e^{-aT}) + v_B T\right]. \tag{12}$$

This may be expressed as the transcendental equation for $\rho = aT$

$$e^{-\rho} + \frac{1}{2}\rho - 1 = 0. \tag{13}$$

Since the ρ is found to be the constant (1.59362..), we obtain

$$aT = \rho = 1.59362\ldots \tag{14}$$

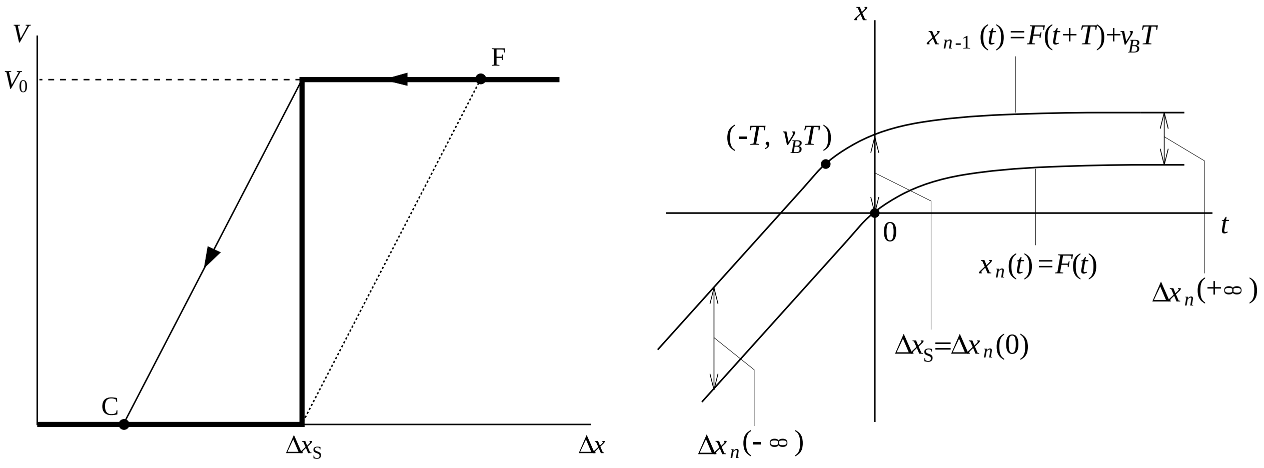

Figure 3: (a) The OV-function (thick line) and a decelerating asymptotic trajectory (thin line with arrows) for the Step Function Model. (b) The position functions $x_n(t)$ and $x_{n-1}(t)$ for the decelerating asymptotic trajectory.

This gives us the a-dependence of T, which was first obtained in Ref. [13].

It is instructive to see a relation between the function $F(t)$ and the decelerating trajectory depicted in Fig. 3. Two curves in Fig. 3(b) correspond to the $(n-1)$-th and n-th vehicles' locations. At $t = 0$ the n-th vehicle's representative point moves into the region I and $F(t)$ is described by an exponential function. Before that time, the function $F(t)$ is linear in t. The curve for the $(n-1)$-th vehicle changes from the linear to the exponential behavior at $t = -T$. It is given via a parallel displacement by the vector $(-T, v_BT)$ from the curve $F(t)$. For the time $t \leq -T$, curves are two parallel straight lines, which implies the headway of the n-th vehicle does not change till that time from the infinite past. The n-th vehicle has the constant velocity V_0 for $t < 0$. This tells us that the n-th vehicle is in the free region for $t \leq -T$, indicated by the point F in Fig. 3(a). It is also easy to observe that at $t = -T$ the $(n-1)$-th vehicle starts to decelerate. As a result the headway of the n-th vehicle decreases; at $t = 0$ it reaches the value $\Delta x_{\rm S}$ and the n-th vehicle starts to decelerate itself.

In this model, the points F and C are both characterized as points which are reached in the infinite future or past. As a traffic flow, we are describing a soliton like solution connecting a half infinite vehicles, running with the velocity v_F and the headway Δx_F, and another half infinite vehicles going into the congested region associated with the point C.

4.2 Single Slope Function Model

In the step function model, the Δx-dependence of the Rondo equation is too simple; T-dependence is not explicit. So we would like to consider a slightly improved model, whose OV-function shown in Fig. 4 has a finite slope. Thus we call this model as the Single Slope Function Model. The OV-function is characterized by the following parameters: f, the slope; V_0, the maximum velocity; $\Delta x_{\rm S}$, the headway for optimal velocity $V_0/2$. From the linear analysis in the paper [1], we know that a homogeneous flow becomes unstable and a congested flow is expected for $2f > a$. This condition is assumed in our analysis here.

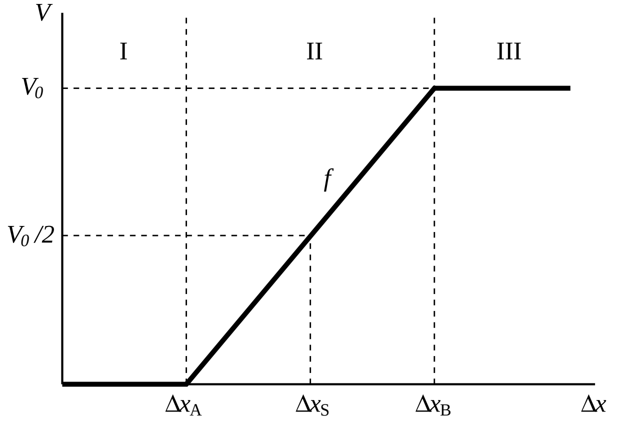

Figure 4: The OV-function for the Single Slope Function Model. f is the gradient in the region II. The function is symmetric with respect to the point $(\Delta x_{\rm S}, V_0/2)$.

The OV-function has sharp bends at

$$\Delta x_{\rm A} = \Delta x_{\rm S} - \frac{V_0}{2f}, \tag{15}$$

$$\Delta x_{\rm B} = \Delta x_{\rm S} + \frac{V_0}{2f}, \tag{16}$$

which divide Δx into three regions, I, II and III, as indicated in Fig. 4.

We would like to find a Rondo function $F(t)$ for a decelerating asymptotic trajectory, along which headway of a vehicle monotonically decreases from $\Delta x_{\rm F}$ to $\Delta x_{\rm C}$. We assume it reaches $\Delta x_{\rm B}$ at $t = -\tau$ and $\Delta x_{\rm A}$ at $t = 0$. The Rondo equation takes of the form,

$$\frac{1}{a}\ddot{F}(t) + \dot{F}(t) = \left\{ \begin{array}{ll} 0 & (t \geq 0) \\ f\left(F(t+T) - F(t) - \delta\right) & (-\tau \leq t \leq 0) \\ V_0 & (t \leq -\tau) \end{array} \right. , \tag{17}$$

subject to the conditions,

$$F(T) - F(0) + v_B T = \Delta x_{\rm A}, \tag{18}$$

$$F(-\tau + T) - F(-\tau) + v_B T = \Delta x_{\rm B}. \tag{19}$$

Here $\delta = \Delta x_A - v_B T$. Note that the time $-\tau$ is not a free parameter. Rather, it should be determined from (19) via solving the Rondo equation.

For regions I and III, the Rondo equation becomes the same as that in the step function model. Therefore, we obtain

$$\dot{F}(t) = \left\{ \begin{array}{ll} \text{const.} \times e^{-at} & \text{(for region I)} \\ V_0 & \text{(for region III).} \end{array} \right. \tag{20}$$

Our purpose in this subsection is to describe a method to find the Rondo function in the region II which correctly interpolates those in (20). To this end, we may introduce a series of functions for each time interval:

$$F(t) = \begin{cases} F^{\mathrm{I}}(t) & (0 \le t) \\ F_1(t) & (-T \le t \le 0) \\ F_2(t) & (-2T \le t \le -T) \\ \quad \vdots & \quad \vdots \\ F^{\mathrm{III}}(t) & (t \le -\tau) \end{cases} \tag{21}$$

The first function $F^{\mathrm{I}}(t) \equiv F_0(t)$ and the last one $F^{\mathrm{III}}(t)$ are for the region I and III, respectively.

Let us find $F^{\mathrm{I}}(t)$ (for $t \ge 0$). It follows from (20) that

$$\dot{F}^{\mathrm{I}}(t) = u_0 e^{-at}, \tag{22}$$

$$F^{\mathrm{I}}(t) = \frac{u_0}{a}\left(1 - e^{-at}\right), \tag{23}$$

where we fix again $F^{\mathrm{I}}(0) = 0$. The n-th vehicle's headway is then given by

$$\Delta x_n(t) = F^{\mathrm{I}}(t+T) + v_B T - F^{\mathrm{I}}(t) = \frac{u_0}{a}(1 - e^{-aT})e^{-at} + v_B T. \tag{24}$$

Since the condition (18) determines the constant u_0

$$u_0 = a\frac{\Delta x_{\mathrm{A}} - v_B T}{1 - e^{-aT}} \equiv \frac{a\delta}{1 - e^{-aT}}, \tag{25}$$

we find the Rondo function for $t \ge 0$ to be

$$F^{\mathrm{I}}(t) = \frac{\delta}{1 - e^{-aT}}\left(1 - e^{-at}\right). \tag{26}$$

This leads to a linear relation between the velocity and the headway,

$$\dot{x}_n = \frac{a}{1 - e^{-aT}}(\Delta x_n - v_B T). \tag{27}$$

In the $t \to \infty$ limit, we find that $\dot{x}_n \to 0$ and $\Delta x_n \to v_B T$.

Now we consider $F_1(t)$ (for $-T \le t \le 0$). In this time interval, the Rondo equation for $F_1(t)$ is expressed as

$$\frac{1}{a}\ddot{F}_1(t) + \dot{F}_1(t) = f(F_0(t+T) - F_1(t) - \delta). \tag{28}$$

in terms of the Rondo function for the region I, $F^{\mathrm{I}}(t) \equiv F_0(t)$. By using the differential operator,

$$\mathcal{D} = \frac{1}{af}\frac{d^2}{dt^2} + \frac{1}{f}\frac{d}{dt} + 1, \tag{29}$$

we may rewrite the above equation as

$$\mathcal{D}F_1(t) = F_0(t+T) - \delta. \tag{30}$$

The general solution may be written as a sum of a particular solution and the solution to the homogeneous equation $\mathcal{D}F_1^{\rm hom}(t) = 0$. It is easy to see that $F_0(t+T)-\delta$ is a particular solution, since the function $F_0(t) \equiv F^{\rm I}(t)$ given in (26) satisfies

$$\mathcal{D}F_0(t) = F_0(t). \tag{31}$$

The exponents γ for a homogeneous solution are

$$\gamma = -\frac{a}{2} \pm i\sqrt{af - \frac{a^2}{4}} \equiv -\frac{a}{2} \pm i\omega. \tag{32}$$

A general solution is given as

$$F_1(t) = F_0(t+T) - \delta + e^{-\frac{a}{2}t}\left(A\sin\omega t + B\cos\omega t\right). \tag{33}$$

The constants A and B are determined as $A = a\delta/\omega$ and $B = 0$, by the requirement that $F_0(t)$ and $F_1(t)$ must be continuous up to the first derivative at $t = 0$. Therefore

$$F_1(t) = \frac{\delta}{1-e^{-aT}}\left(1 - e^{-a(t+T)}\right) - \delta + \frac{a\delta}{\omega}e^{-\frac{a}{2}t}\sin\omega t, \tag{34}$$

and the headway and the velocity for the n-th vehicle is given as

$$\begin{aligned}\Delta x_n(t) &= F_0(t+T) - F_1(t) + v_B T = \Delta x_{\rm A} - \frac{a\delta}{\omega}e^{-\frac{a}{2}t}\sin\omega t,\\ \dot{x}_n(t) &= \dot{F}_1(t) = \frac{a\delta}{e^{aT}-1}e^{-at} + \frac{a\delta}{\omega}e^{-\frac{a}{2}t}\left(\omega\cos\omega t - \frac{a}{2}\sin\omega t\right).\end{aligned} \tag{35}$$

We would now like to give general formula for $F_k(t)$ (for $t \in I_k = [-kT, -(k-1)T]$) with $k > 1$. Suppose that $F_k(t)$ for $t \in I_k$ is known to us and we are trying to find $F_{k+1}(t)$ for $t \in I_{k+1}$. $F_{k+1}(t)$ satisfies the second order linear differential equation,

$$\mathcal{D}F_{k+1}(t) = F_k(t+T) - \delta, \tag{36}$$

with boundary conditions;

$$\begin{aligned}F_{k+1}(-kT) &= F_k(-kT),\\ \dot{F}_{k+1}(-kT) &= \dot{F}_k(-kT),\end{aligned} \tag{37}$$

while $F_k(t)$ satisfies a similar equation,

$$\mathcal{D}F_k(t) = F_{k-1}(t+T) - \delta. \tag{38}$$

The function $F_k(t)$ describes the behavior of the n-th vehicle only for $t \in I_k$. However we will find it useful to define the function by the relation (38) even outside the interval I_k. The function used outside the interval will be denoted as $\widetilde{F}_k(t)$. The difference of (36) and (38) gives us the following equation for $t \in I_{k+1} = [-(k+1)T, -kT]$,

$$\mathcal{D}\left(F_{k+1}(t) - \widetilde{F}_k(t)\right) = F_k(t+T) - \widetilde{F}_{k-1}(t+T) \quad (k \geq 1). \tag{39}$$

From (30) and (31) we find

$$\mathcal{D}\left(F_1(t)-\widetilde{F}_0(t)\right)=F_0(t+T)-\widetilde{F}_0(t)-\delta=\delta\left(e^{-at}-1\right), \tag{40}$$

for $t \in I_1=[-T,0]$.

By using the function $G_k(t)$ defined in the relation,

$$F_{k+1}(t)=\widetilde{F}_k(t)+G_{k+1}(t+kT), \tag{41}$$

(39) and (40) are rewritten into the following equations for $-T \le t \le 0$,

$$\mathcal{D}G_{k+1}(t)=G_k(t) \qquad (k \ge 1), \tag{42}$$

$$\mathcal{D}G_1(t)=\delta\left(e^{-at}-1\right)\equiv G_0(t). \tag{43}$$

Note that $G_0(t)$ defined in (43) satisfies $\mathcal{D}G_0(t)=G_0(t)$. The conditions (37) become $G_k(0)=0$ and $\dot{G}_k(0)=0$ (for $k \ge 1$).

The Rondo function $F(t)$ for the region II is given as a sum of $G_k(t)$,

$$F^{\mathrm{II}}(t)=F_0(t)+\sum_{k\ge 0}\theta(-t-kT)G_{k+1}(t+kT), \tag{44}$$

for $t>-\tau$. In the appendix B we will give general solutions to differential equations (42) and (43). $G_1(t)$ from the appendix,

$$G_1(t)=G_0(t)+\frac{a\delta}{\omega}e^{-\frac{a}{2}t}\sin\omega t=\delta\left(e^{-at}-1\right)+\frac{a\delta}{\omega}e^{-\frac{a}{2}t}\sin\omega t, \tag{45}$$

is consistent to (34). Similarly $G_2(t)$ is given as

$$G_2(t)=G_1(t)-\frac{a\delta}{\omega}\frac{2f}{4f-a}e^{-\frac{a}{2}t}\left\{\omega t\cos\omega t-\sin\omega t\right\}. \tag{46}$$

So $F_2(t)$ for $t \in I_2=[-2T,-T]$ becomes

$$\begin{aligned} F_2(t) &= \widetilde{F}_1(t)+G_2(t+T) \\ &= \widetilde{F}_1(t)+\delta\left(e^{-a(t+T)}-1\right)+\frac{a\delta}{\omega}e^{-\frac{a}{2}(t+T)}\sin\omega(t+T) \\ &\quad -\frac{a\delta}{\omega}\frac{2f}{4f-a}e^{-\frac{a}{2}(t+T)}\left\{\omega(t+T)\cos\omega(t+T)-\sin\omega(t+T)\right\}, \end{aligned} \tag{47}$$

while the headway for the n-th vehicle is

$$\begin{aligned} \Delta x_n(t) &= \Delta x_{\mathrm{A}}-\frac{a\delta}{\omega}e^{-\frac{a}{2}t}\sin\omega t \\ &\quad +\frac{a\delta}{\omega}\frac{2f}{4f-a}e^{-\frac{a}{2}(t+T)}\left\{\omega(t+T)\cos\omega(t+T)-\sin\omega(t+T)\right\}. \end{aligned} \tag{48}$$

The general formula in appendix B may be used further to generate $F_3, F_4, \cdots$, needed to describe the trajectory in the region II.

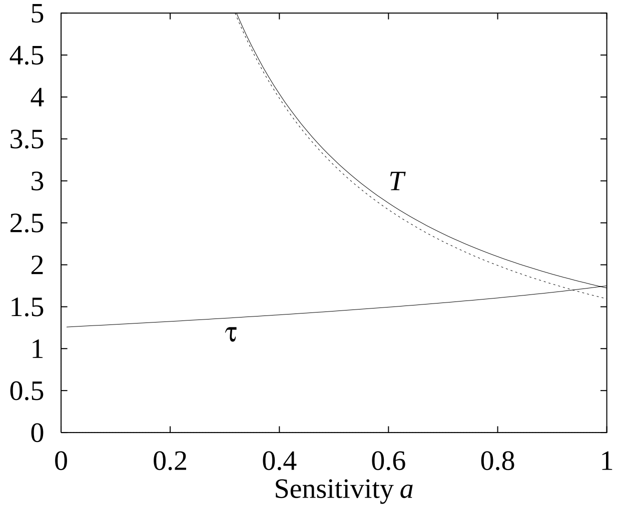

Figure 5: Sensitivity dependence of T and τ for the Single Slope Function Model. The condition, $T \geq \tau$, is assumed, which is satisfied for $a \leq 0.98857\ldots$ The dotted line shows the a-T relation for the Step Function Model.

Let us consider the region III. At $t = -\tau$, the function (44) for the region II must be continuously connected to $F^{\mathrm{III}}(t)$ including their first derivatives. This condition yields $F^{\mathrm{III}}(t)$ for $t \leq -\tau$ as

$$F^{\mathrm{III}}(t) = V_0\ (t+\tau) + F^{\mathrm{II}}(-\tau). \tag{49}$$

The continuity condition for the first derivative requires also that

$$\dot{F}^{\mathrm{II}}(-\tau) = \dot{F}^{\mathrm{III}}(-\tau) \equiv V_0. \tag{50}$$

This completes our construction of an asymptotic trajectory.

Now let us find the a-dependence of T for the present model. The time $-\tau$ may be determined by the condition (19), $F(-\tau+T) - F^{\mathrm{II}}(-\tau) + v_B T = \Delta x_B$; then Eq. (50) gives us a relation between a and T. By using (44) for $F^{\mathrm{II}}(-\tau)$, concrete expressions of (19) and (50) may be obtained. For $-T \leq -\tau$, $F^{\mathrm{II}}(-\tau)$ is simply given by $F_1(-\tau)$ and the above conditions are expressed as:

$$\frac{a\delta}{\omega} e^{\frac{a}{2}\tau} \sin\omega\tau = \Delta x_{\mathrm{B}} - \Delta x_{\mathrm{A}} \equiv \frac{V_0}{f}, \tag{51}$$

$$\frac{a\delta}{e^{aT}-1} e^{a\tau} + \frac{a\delta}{\omega} e^{\frac{a}{2}\tau} \left(\omega\cos\omega\tau + \frac{a}{2}\sin\omega\tau\right) = V_0. \tag{52}$$

The requirement of symmetry, $\Delta x_n(+\infty) + \Delta x_n(-\infty) = 2\Delta x_{\mathrm{S}}$, mentioned in section 3 becomes $v_B T + (V_0 + v_B)T = 2\Delta x_{\mathrm{S}}$. This relation and Eq. (16) allow us to express $\delta = \Delta x_A - v_B T$ as,

$$\delta = (fT-1)\frac{V_0}{2f}. \tag{53}$$

Finally, we reach to the coupled equations which determine T and τ for given slope f and sensitivity a:

$$\left\{ \begin{array}{l} (fT-1)e^{\frac{a}{2}\tau}\sin\omega\tau = \dfrac{2\omega}{a}, \\ \left(e^{aT}-1\right)\left[\left(f-\dfrac{a}{2}\right)\sin\omega\tau - \omega\cos\omega\tau\right] = \omega e^{\frac{a}{2}\tau}, \end{array} \right. \tag{54}$$

where ω is given in Eq. (32). For $f = 1.0$, Eq. (54) is solved numerically to give the a-dependence of T and τ as shown in Fig. 5. Since we used $F_1(t)$ for $F^{II}(t)$, Eq. (54) is valid only for $\tau \leq T$ (τ coincides with T when $a = 0.98857..$ at $\tau = T = 1.74027..$).

We observe in Fig. 5 that T behaves as $1/a$ for small a: this implies that, for congested flows to be formed, the delay T must be larger for less sensitive drivers. In the limit of $f \to \infty$, the present model reduces to the Step Function Model, in which $aT = \rho$ and $\tau = 0$. This may be confirmed with Eq. (54) since aT reaches a constant, $\rho = 1.59362..$, and $a\tau$ behaves like $2a/(f\rho)$ when a/f goes to zero.[5]

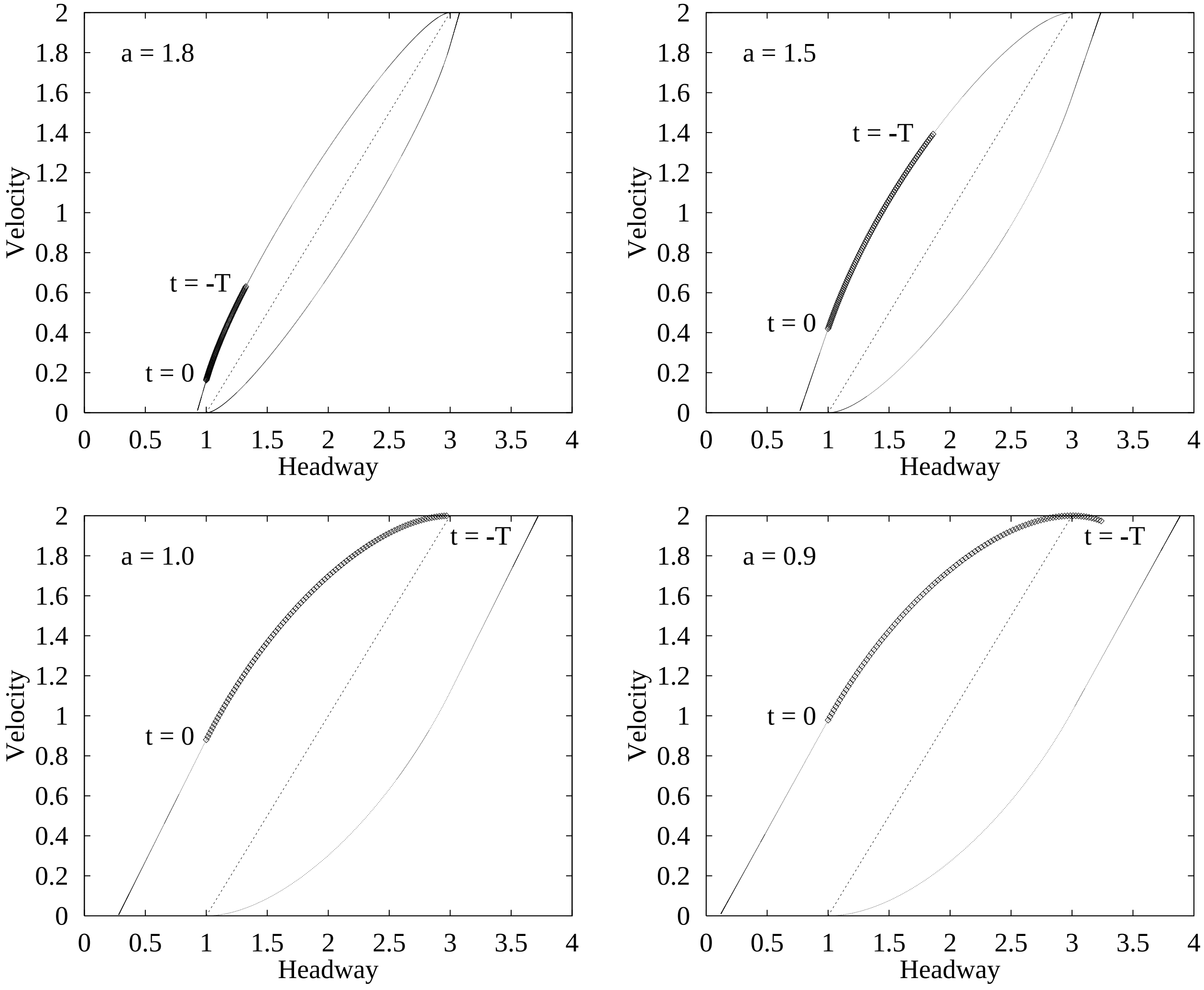

Figure 6: Thin curves show "limit cycles" for the Single Slope Function Model obtained from simulations with (a) $a = 1.8$, (b) $a = 1.5$, (c) $a = 1.0$ and (d) $a = 0.9$. Trajectories generated from $F_1(t)$ for $t \in [-T, 0]$ are drawn with thick curves. The curves inside the region II ($1 < \Delta x < 3$) are parts of asymptotic trajectories. The dotted line shows the OV-function with $f = 1.0$, $V_0 = 2.0$ and $\Delta x_{\rm S} = 2.0$.

In order to see the validity of our approach, let us compare our results and trajectories obtained by simulations. In Fig. 6, thick curves show parts of the asymptotic trajectories, to be determined by the function $F_1(t)$, for $a = 1.8,\ 1.5$ ($\tau > T$), $a = 1.0$ ($\tau \sim T$) and $a = 0.9$ ($\tau < T$). These curves are to be compared with numerical simulations shown as thin curves. The function $F_1(t)$ is enough to give an asymptotic trajectory for $a \leq 0.98857..$, as mentioned above. It is expected that when a gets closer to its critical value ($a_{\text{critical}} = 2f = 2.0$, in this case), we need functions $F_k(t)$ with higher k to form an entire trajectory.

---

[5] Note that Eq. (54) may be rewritten in terms of rescaled variables aT, $a\tau$ and a/f.

There appears a flat trajectory again in the region III. As in the Step Function Model, it takes time T for a vehicle to move on the flat trajectory and there is only one vehicle traveling on this interval.

4.3 Double Slope Function Model

The OV-function for the single slope model has flat regions I and III like the step function model. For those regions the Rondo equation does not depend on $F(t+T)$: a vehicle does not react to the motion of the preceding one. This motivates us to consider a more realistic model with an OV-function which has non-zero gradient for any headway.

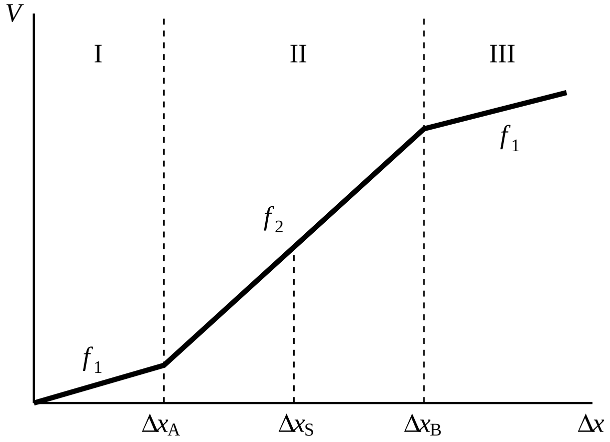

Figure 7: The OV-function for the Double Slope Function Model, which is symmetric with respect to the point $(\Delta x_S, V(\Delta x_S))$. It has the gradient f_1 (f_2) in the regions I and III (II).

The OV-function has a slope f_1 in regions I and III, and f_2 in region II (see Fig. 7):

$$V(\Delta x) = \begin{cases} f_1 \Delta x & \Delta x \leq \Delta x_A \quad \text{(region I)} \\ f_2 \left[\Delta x - (1-\kappa)\Delta x_A\right] & \Delta x_A \leq \Delta x \leq \Delta x_B \quad \text{(region II)} \\ f_1 \left[\Delta x + (\kappa^{-1} - 1)(\Delta x_B - \Delta x_A)\right] & \Delta x_B \leq \Delta x \quad \text{(region III).} \end{cases} \tag{55}$$

where $\kappa = f_1/f_2$. Obviously this function is symmetric around $(\Delta x_S, V(\Delta x_S))$, where Δx_S is the middle point of the region II. Here we should note that the sensitivity a must satisfy $f_1 < a/2 < f_2$ for generation of the congestion in this model, since the homogeneous flow is expected to be linearly unstable only in the region II.

As in the previous subsection, we assume that the headway reaches Δx_B at $t = -\tau$ and Δx_A at $t = 0$. The solution of the Rondo equation (6) must satisfy the conditions (18), (19). The Rondo function $F(t)$ for three regions will be denoted as follows;

$$F(t) = \begin{cases} F^{\mathrm{I}}(t) & (0 \le t) \\ F^{\mathrm{II}}(t) & (-\tau \le t \le 0) \\ F^{\mathrm{III}}(t) & (t \le -\tau). \end{cases} \tag{56}$$

For $F^{\mathrm{I}}(t)$ $(t \ge 0)$, the Rondo equation is given by

$$\mathcal{D}_1 F^{\mathrm{I}}(t) = F^{\mathrm{I}}(t+T) + v_B T, \tag{57}$$

where

$$\mathcal{D}_1 = \frac{1}{af_1}\frac{d^2}{dt^2} + \frac{1}{f_1}\frac{d}{dt} + 1. \tag{58}$$

To find a solution to the homogeneous equation $\mathcal{D}_1 F^{\mathrm{I}}_{\mathrm{hom}}(t) = F^{\mathrm{I}}_{\mathrm{hom}}(t+T)$, we use the ansatz $F^{\mathrm{I}}_{\mathrm{hom}}(t) \sim e^{\gamma t}$ which gives an equation for the exponent γ,

$$\frac{\gamma^2}{a} + \gamma = f_1(e^{\gamma T} - 1). \tag{59}$$

As long as the condition $f_1 < 1/T$ holds,[6] there are two real solutions: the negative $-\gamma_{\mathrm{in}}$ and the positive one γ_{out}. Because of the asymptotic behavior, $\dot{F}(t) \to v_{\mathrm{C}}$ as $t \to +\infty$, only the exponent $-\gamma_{\mathrm{in}}$ is relevant to the function $F^{\mathrm{I}}(t)$. Adding a particular solution of (57), we obtain the solution subject to conditions (18) and $F(0) = 0$ as

$$F^{\mathrm{I}}(t) = v_{\mathrm{C}} t + (\Delta x_{\mathrm{A}} - \Delta x_{\mathrm{C}}) \frac{1 - e^{-\gamma_{\mathrm{in}} t}}{1 - e^{-\gamma_{\mathrm{in}} T}}. \tag{60}$$

By calculating $\Delta x_n(t)$ and $\dot{x}_n(t)$ from (60),

$$\begin{aligned} \Delta x_n(t) &= \Delta x_{\mathrm{C}} + (\Delta x_{\mathrm{A}} - \Delta x_{\mathrm{C}}) e^{-\gamma_{\mathrm{in}} t}, & (61) \\ \dot{x}_n(t) &= v_{\mathrm{C}} + (\Delta x_{\mathrm{A}} - \Delta x_{\mathrm{C}}) \frac{\gamma_{\mathrm{in}}}{1 - e^{-\gamma_{\mathrm{in}} T}} e^{-\gamma_{\mathrm{in}} t}, & (62) \end{aligned}$$

we obtain a linear trajectory given by

$$\dot{x}_n(t) - v_{\mathrm{C}} = \frac{\gamma_{\mathrm{in}}}{1 - e^{-\gamma_{\mathrm{in}} T}} \left(\Delta x_n(t) - \Delta x_{\mathrm{C}}\right). \tag{63}$$

In the region II the function $F^{\mathrm{II}}(t)$ is divided into $F_k(t)$'s for $t \in I_k = [-kT, -(k-1)T]$ as was done in the previous subsection. We may now study the Rondo equation,

$$\mathcal{D}_2 F_k(t) = F_{k-1}(t+T) + v_B T - (1-\kappa)\Delta x_{\mathrm{A}} \qquad (k \ge 1), \tag{64}$$

where $F_0(t) \equiv F^{\mathrm{I}}(t)$ and $\mathcal{D}_2$ is $\mathcal{D}_1$ with f_1 replaced by f_2: $\mathcal{D}_2 = \mathcal{D}_1 - (1-\kappa)(\mathcal{D}_1 - 1)$. In terms of $\mathcal{D}_2$, equation (57) becomes

$$\mathcal{D}_2 F_0(t) = F_0(t+T) + v_B T - (1-\kappa)\Delta x_n(t), \tag{65}$$

where $\Delta x_n(t)$ is given by (61).

---

[6] When a congested flow is realized in this model, this condition is satisfied trivially.

The basic technique in the last subsection may be used to solve (64) with a slight modification. Let us define $G_k(t)$'s with $F_{k+1}(t) = \tilde{F}_k(t) + G_{k+1}(t+kT)$, which satisfy the equations,

$$\mathcal{D}_2 G_{k+1}(t) = G_k(t) \qquad (k \geq 1), \tag{66}$$

$$\mathcal{D}_2 G_1(t) = \delta \left(e^{-\gamma_{\rm in} t} - 1\right) \equiv G_0(t), \tag{67}$$

where $\delta = (1-\kappa)(\Delta x_{\rm A} - \Delta x_{\rm C})$. The boundary conditions are $G_k(0) = \dot{G}_k(0) = 0$ for $k \geq 1$. In solving these, we may use again the formula given in the appendix B. Once we find the series of $G_k(t)$, we obtain the function $F^{\rm II}(t)$ by the relation (44). Further we can determine the time $-\tau$ by the condition (19), $F(-\tau+T) - F^{\rm II}(-\tau) + v_B T = \Delta x_B$.

In the region III ($t \leq -\tau$), the Rondo equation take the form,

$$\mathcal{D}_1 F^{\rm III}(t) = F^{\rm X}(t+T) + v_B T + (\kappa^{-1} - 1)(\Delta x_{\rm B} - \Delta x_{\rm A}), \tag{68}$$

where $F^{\rm X}(t+T)$ is $F^{\rm II}(t+T)$ for $-\tau \leq t+T \leq -\tau+T$ and $F^{\rm III}(t+T)$ for $t+T \leq -\tau$. The solution must be continuously connected to $F^{\rm II}(t)$ including the first derivative at $t = -\tau$. Eq. (68) can be solved by the same manner as in the region II, though homogeneous solutions to the equation (68) include the hyperbolic functions instead of the trigonometric functions.

The logic at the end of section 3 may be used to get a better perspective on what we have discussed up to now, and it will leads us to find the a-dependence of T. First, with a given slope T^{-1}, we draw the straight line through the point S. The value of $-v_B$ and the coordinates of C and F are given in terms of T and the parameters in the OV-function,

$$v_{\rm C} = \frac{f_1 T}{1 - f_1 T} v_B, \quad \Delta x_{\rm C} = \frac{v_B T}{1 - f_1 T}, \tag{69}$$

$$\begin{aligned} v_{\rm F} &= \frac{f_1 v_B T + f_1(\kappa^{-1} - 1)(\Delta x_{\rm B} - \Delta x_{\rm A})}{1 - f_1 T}, \\ \Delta x_{\rm F} &= \frac{v_B T + f_1 T(\kappa^{-1} - 1)(\Delta x_{\rm B} - \Delta x_{\rm A})}{1 - f_1 T}, \end{aligned} \tag{70}$$

and

$$-v_B = \left(f_1 - \frac{f_2 T + 1}{2T}\right) \Delta x_A + \frac{f_2 T - 1}{2T} \Delta x_B. \tag{71}$$

In solving the Rondo equation, we have introduced a parameter τ determined by Eq. (19). Using this τ and v_B expressed as Eq. (71), we obtain one parameter family of (a-dependent) solution to the Rondo equation. Then, we find an appropriate value of a for a given T by the requirement that the asymptotic trajectory connects C and F: $\dot{F}^{\rm III}(-\infty) = v_{\rm F}$.

In Fig. 8, we show trajectories from our analytic study and a computer simulation for the double slope model. We have chosen a particular value for a so that $\tau = T$ and we used the Rondo function for $t > -\tau - T$ to draw the part of the decelerating asymptotic trajectory. Clearly the Rondo function reproduces the trajectory obtained via a computer simulation.

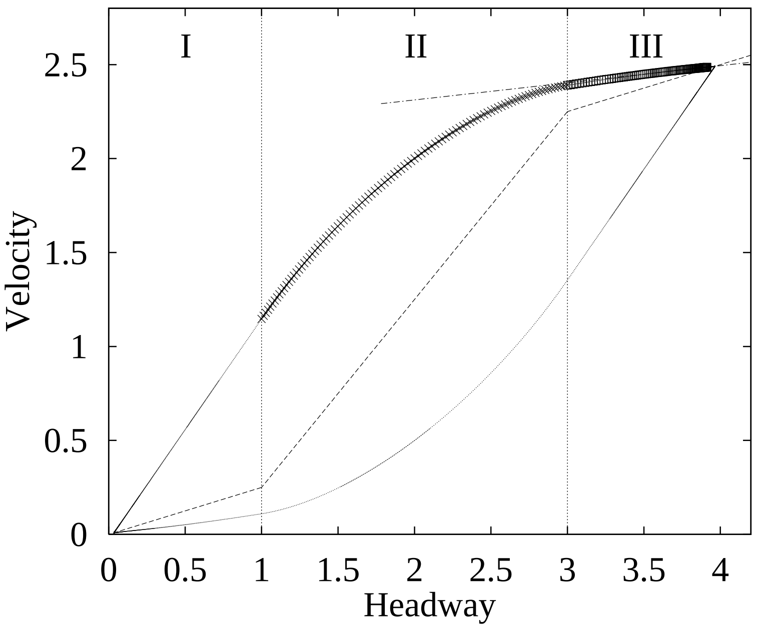

Figure 8: Trajectories for the Double Slope Model. Thin curve shows "limit cycle" from simulation with $a = 1.13124$ when $T = \tau = 1.58331$. The analytical solution is drawn with thick curve. The dotted-dashed line shows the trajectory expressed by the exponential function with index γ_{out}. The dotted line shows the OV-function with $f_1 = 0.25$, $f_2 = 1.0$, $\Delta x_{\text{A}} = 1.0$ and $\Delta x_{\text{B}} = 3.0$.

By the procedure described in this subsection, we may easily obtain the remaining part of the asymptotic trajectory. When this is carried out, we expect that it reaches to the point F in the infinite past. In the following we will give another argument to support this expectation. The Rondo equation for $t < -\tau - T$ in the region III may be solved with exponential functions plus a particular solution, as for the region I: the function $F^{\text{III}}(t)$ is the sum of a term linear in t and exponential functions. In the limit $t \to -\infty$, only the linear term survives expressing that vehicles have the velocity for a free region, v_{F}; the exponents satisfy Eq. (59) and have positive real parts so that exponential functions vanish as $t \to -\infty$.

It would be appropriate to explain how solutions to Eq. (59) are distributed on the complex γ-plane. Without going into the details, here we only quote features relevant to our arguments. There is only one solution with negative real part, it actually a real solution $-\gamma_{\text{in}}$. Other solutions have positive real parts, which are relevant when $t \sim -\infty$. There is only one real solution, γ_{out}; there are complex pair solutions with their real parts larger than γ_{out}. Since γ_{out} has the smallest positive real part, it dominates among exponential functions when $t \to -\infty$. Thus for very large negative t, the function $F^{\text{III}}(t)$ may be approximated by the exponential functions with γ_{out}. In the region I, we found that the decelerating asymptotic trajectory is linear on the Δx-v plane owing to the exponential term in $F^{\text{I}}(t)$. Similarly, the approximated $F^{\text{III}}(t)$ define a line on the Δx-v plane, starting the point F as shown in Fig. 8. We observe that this line is actually the tangent line to the trajectory at the point F.

The absence of the flat region is directly related to our observation that the point F in reached only in the infinite past. If we consider the limit to have a flat region, $f_1 = 0$, we only have a negative solution $\gamma_{\text{in}} = -a$. When we would like to consider the OV-model applied for a realistic situation, the relevant OV-function may be approximately realized by a piece-wise linear function. Since it is unlikely that the function has a flat region, the above feature of the double slope model must be generic.

5 Trajectories around Cusps

In the last section, we discussed asymptotic trajectories in models with piece-wise linear OV-functions. The asymptotic trajectories can be realized only when the number of vehicles becomes infinite. In computer simulations in Refs.[1, 2, 3], a finite number of vehicles run around a circuit; a vehicle goes through all the free and congested regions in a finite time. The Rondo equation probably has solutions even for such situations. Though we have not worked out how to obtain entire trajectories for such vehicles, we are able to discuss parts of the trajectories around the points C or F. We are going to discuss this subject in this section.

To make our explanation concrete, we take a trajectory around the end point C. In a congested region, all the vehicles have almost the same velocity. When a vehicle is about to reach a congested region, its velocity would be slightly different from v_{C} and the function $F(t)$ may be written as $F(t) = v_{\text{C}}t + \xi(t)$. We take a linear approximation for an OV-function $V(\Delta x)$[7] around the point $(\Delta x_{\text{C}}, v_{\text{C}})$,

$$V(\Delta x) \simeq f_{\text{C}}(\Delta x - \Delta x_{\text{C}}) + v_{\text{C}}. \tag{72}$$

Since $(v_B + v_{\text{C}})T = \Delta x_{\text{C}}$, the Rondo equation (6) becomes a linear difference-differential equation for $\xi(t)$,

$$\frac{\ddot{\xi}(t)}{a} + \dot{\xi}(t) = f_{\text{C}}(\xi(t+T) - \xi(t)). \tag{73}$$

For the ansatz $\xi(t) = e^{\gamma t}$, we find an equation for the exponent γ,

$$\frac{\gamma^2}{a} + \gamma = f_{\text{C}}(e^{\gamma T} - 1). \tag{74}$$

As long as $f_{\text{C}} < 1/T$, there are two real solutions: the negative, $-\gamma_{\text{in}}$, and the positive one, γ_{out}.[8]

Trajectories considered here cross (at $t = 0$) the OV-function at points slightly different from C: we denote their coordinates by $(\Delta x, v) = (\Delta x_{\text{C}} + \delta v/f_{\text{C}}, v_{\text{C}} + \delta v)$. We find the solution for $F(t)$ as,

$$F(t) = v_{\text{C}}t + \frac{-\gamma_{\text{out}}^2 e^{-\gamma_{\text{in}}t} + \gamma_{\text{in}}^2 e^{\gamma_{\text{out}}t}}{\gamma_{\text{in}}\gamma_{\text{out}}(\gamma_{\text{in}} + \gamma_{\text{out}})}\delta v. \tag{75}$$

We may find $\Delta x_n(t)$ and $v_n(t)$ from this solution

$$\Delta x_n(t) = \Delta x_{\text{C}} + \frac{(a - \gamma_{\text{in}})\gamma_{\text{out}} e^{-\gamma_{\text{in}}t} + (a + \gamma_{\text{out}})\gamma_{\text{in}} e^{\gamma_{\text{out}}t}}{a(\gamma_{\text{in}} + \gamma_{\text{out}})}\frac{\delta v}{f_{\text{C}}}, \tag{76}$$

---

[7] Here as an OV-function we have in mind a smooth, but not necessarily a piece-wise linear, function.

[8] We ignored complex solutions in this approximation since the real of those solutions are larger than γ_{out}. See the discussion in the last section.

$$v_n(t) = v_{\mathrm{C}} + \frac{\gamma_{\mathrm{out}} e^{-\gamma_{\mathrm{in}} t} + \gamma_{\mathrm{in}} e^{\gamma_{\mathrm{out}} t}}{\gamma_{\mathrm{in}} + \gamma_{\mathrm{out}}} \delta v. \tag{77}$$

By eliminating the time t, we find the equation for the trajectory around the point C,

$$\left[\frac{a f_{\mathrm{C}}(\Delta x - \Delta x_{\mathrm{C}}) - (a - \gamma_{\mathrm{in}})(v - v_{\mathrm{C}})}{\gamma_{\mathrm{in}} \delta v}\right]^{\gamma_{\mathrm{in}}} \left[\frac{(a + \gamma_{\mathrm{out}})(v - v_{\mathrm{C}}) - a f_{\mathrm{C}}(\Delta x - \Delta x_{\mathrm{C}})}{\gamma_{\mathrm{out}} \delta v}\right]^{\gamma_{\mathrm{out}}} = 1. \tag{78}$$

This curve shown in Fig. 9 has two asymptotes through C with slopes $a f_{\mathrm{C}}/(a - \gamma_{\mathrm{in}})$ and $a f_{\mathrm{C}}/(a + \gamma_{\mathrm{out}})$, which correspond to the decelerating and accelerating asymptotic trajectories, respectively.

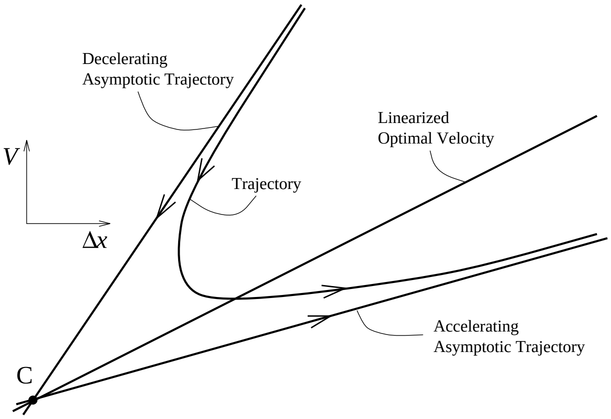

Figure 9: A trajectory in linear approximation for a vehicle passing through the congested region with a finite size. It has two asymptotes, accelerating and decelerating asymptotic trajectories. The time development is indicated with arrows.

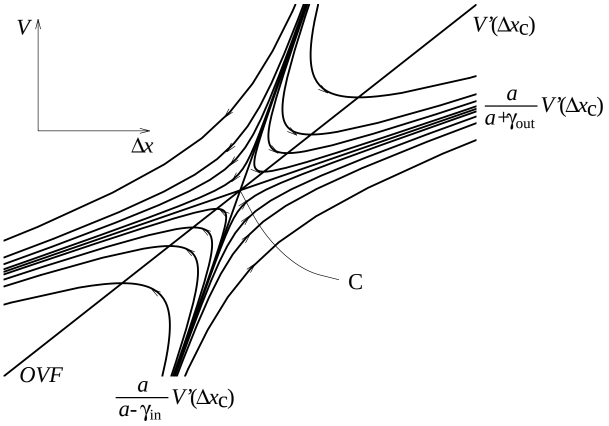
V
$V'(\Delta x_C)$
$\frac{a}{a+\gamma_{out}} V'(\Delta x_C)$
Δx
C
OVF
$\frac{a}{a-\gamma_{in}} V'(\Delta x_C)$

Figure 10: The flow diagram around the point C obtained by the linear approximation. Two asymptotes are asymptotic trajectories.

Two asymptotes of (78) divide the Δx-v plane into four areas. In Fig. 10, curves are shown for solutions to Eq. (73) with various initial conditions: the point C is a saddle point. The linear analysis applies to the point F as well, so curves in the left-lower region would describe the behavior of vehicles close to a free region.

The condition, $(v(t)-v_{\mathrm{C}})/v_{\mathrm{C}} << 1$, helps us to evaluate t_{C}, the time interval a vehicle would spend around the point C;

$$t^2 << \frac{2}{\gamma_{\mathrm{in}}\gamma_{\mathrm{out}}}\frac{v_{\mathrm{C}}}{\delta v} \sim t_{\mathrm{C}}^2. \tag{79}$$

The time t_{C} is related to the length of a congested region L_{C} and the number of vehicles in this region N_{C} as follows,

$$N_{\mathrm{C}} = \frac{t_{\mathrm{C}}}{T}, \qquad L_{\mathrm{C}} = N_{\mathrm{C}}\Delta x_{\mathrm{C}} = \Delta x_{\mathrm{C}}\frac{t_{\mathrm{C}}}{T} \tag{80}$$

Therefore the size of a congested region is larger for smaller δv.

6 Summary and Discussion

We have investigated the repetitive pattern formation observed in a computer simulation from an analytical point of view. The Rondo approach was proposed to describe the repetitive pattern. In addition to a and $V(\Delta x)$, the difference-differential equation for the Rondo function $F(t)$ contains two macroscopic parameters, T and v_B, which specify the motion of a global pattern. In this paper we mainly paid our attention to Rondo functions for asymptotic trajectories. The Rondo equation was solved for three simple models with piece-wise linear OV-functions. In order to determine the a-dependence of T and v_B, we gave analytic expressions for Rondo functions. We would like to emphasize that the concept of asymptotic trajectory plays a key role to determine the a-dependence of T and v_B. As a first step to understand more realistic situations, we have studied some trajectories around cusps.

In the following we discuss three questions related to the Rondo approach: (1) extension to OV-models with asymmetric OV-functions; (2) more on realistic trajectories; (3) possibility to find the Rondo function *forward* in time.

Studying more realistic models, we may encounter an asymmetric OV-function. We explain how our procedure developed in this paper may be extended to such situations. Even with an asymmetric OV-function, we may define the concept of accelerating and decelerating asymptotic trajectories. When the symmetry is absent, accelerating and decelerating asymptotic trajectories are not related each other and must be found independently. The condition that both of them share the same end points C and F will determine the a-dependence of T.

Even though we have mainly studied asymptotic trajectories, the Rondo equation itself must be applicable for any repetitive motion of vehicles. On the other hand, as we have observed for piece-wise linear models, the difference between asymptotic trajectories and the results of computer simulations are very small. Therefore whether we would like to obtain a realistic trajectory out of the Rondo approach or not is very much dependent of our purpose.

The Rondo equation gives us a functional relation which may be written as,

$$F(t+T) = \mathcal{P}[F(t), \dot{F}(t), \ddot{F}(t); a, v_B, T], \tag{81}$$

with three parameters a, v_B and T. When we know the function $F(t)$ for the time interval $t \in [t_0, t_0+T]$, there are two ways to use the above equation: (1) substituting this on the r.h.s., we find $F(t)$ for $t \in [t_0 + T, t_0 + 2T]$; (2) the same information may be used on the l.h.s. to have a differential equation for $F(t)$ on the interval $t \in [t_0 - T, t_0]$. Although the former sounds much easier, we have been able to use the Rondo equation only in the latter manner. Here we would explain the reason why it was so.

Now let us consider, for concrete, a decelerating asymptotic trajectory in the double slope model. In order to use Eq. (81) in the approach (1), we need the Rondo function describing a part of the asymptotic trajectory coming out of F; the rest of the asymptotic trajectory may be obtained just by differentiating the initial function repeatedly. So the initial Rondo function is of vital importance.

Since the OV-function is symmetric, the transcendental equation (59) may be used to find the initial Rondo function. Let us remember how solutions are distributed. There are only two real solutions, $-\gamma_{\rm in} < 0$ and $\gamma_{\rm out} > 0$, and infinitely many complex solutions whose real parts are larger than $\gamma_{\rm out}$. The initial Rondo function is a linear combination of infinitely many exponential functions with $\mathrm{Re}(\gamma) > 0$. Therefore it contains infinitely many coefficients, which must be determined to give an asymptotic trajectory with properties described in section 3. To find an asymptotic trajectory in this way, we probably need some new techniques.

In this paper we have considered the repetitive pattern in traffic flow. Such repetitive structure is also observed in various phenomena, and we believe that our approach may be helpful to understand them.

Appendix

A Asymptotic trajectory is symmetric

In this paper we have used the following property of an asymptotic trajectory: $(\Delta x_{\rm C}, v_{\rm C})$ and $(\Delta x_{\rm F}, v_{\rm F})$ are at symmetric positions for OV-function symmetric around a point S. Here we would like to give a proof of the above claim for an OV-function symmetric with respect to the point S.

Suppose an OV-function function and a sensitivity are given. Our Rondo equation contains two parameters T and v_B;

$$\frac{1}{a}\ddot{F}(t) + \dot{F}(t) = V(F(t+T) - F(t) + v_B T). \qquad (82)$$

If we could find a solution $F(t)$ for the equation, this means that, for the OV-function and the sensitivity a, corresponding pattern with the delay T and the backward velocity v_B may be realized.

The OV-function is taken to be an odd function around the point $\mathrm{S}(\Delta x_{\rm S}, v_{\rm S})$. This assumption is expressed with an odd function $W(-x) = -W(x)$ as follows,

$$V(\Delta x) = v_{\rm S} + W(\Delta x - \Delta x_{\rm S}). \qquad (83)$$

By putting this form to the Rondo equation, it now looks like,

$$\frac{1}{a}\ddot{F}(t) + \dot{F}(t) = v_{\rm S} + W(F(t+T) - F(t) + v_B T - \Delta x_{\rm S}). \qquad (84)$$

We assume that a solution to the Rondo equation has been found. It gives a trajectory on the Δx-v plane, whose coordinate we denote as $(\Delta x_1(t), v_1(t))$. They are expressed with the function $F(t)$ as follows,

$$v_1(t) = \dot{F}(t), \qquad \Delta x_1(t) = F(t+T) - F(t) + v_B T. \tag{85}$$

By using the fact that W is odd, it is easily shown that $(\Delta x_2(t), v_2(t))$ given below satisfies the Rondo equation as well.

$$v_2(t) = \dot{\bar{F}}(t), \qquad \Delta x_2(t) = \bar{F}(t+T) - \bar{F}(t) + v'_B T, \tag{86}$$

where $\bar{F}(t) \equiv 2v_{\rm S} t - F(t)$ and $v'_B T \equiv -2v_{\rm S} T - v_B T + 2\Delta x_{\rm S}$.

It is also easy to see that $(\Delta x_1(t), v_1(t))$ and $(\Delta x_2(t), v_2(t))$ are symmetric with respect to the point S. Therefore if the former defines a trajectory from a free to a congested region, the latter defines that for opposite direction.

Here we emphasize that two trajectories have different backward velocities but with the same delay time T.

In computer simulations, we observe that a pattern of a congested flow is characterized with two parameters T and v_B; both regions, connecting free to congested or congested to free, moves with the same backward velocity v_B. So two trajectories connecting free and congested regions must have the same parameters. This must be also true for an asymptotic trajectory. Therefore v'_B must be equal to v_B itself. This implies that two trajectories discussed above form a closed trajectory. Thus we may conclude the following: 1) solutions expressed by $F(t)$ and $\bar{F}(t)$ satisfy the Rondo equation with the same parameters T and v_B ; 2) the two points on the OV-function connected by trajectories are symmetric with respect to the point S; 3) the straight line through the two points includes the point S.

B General formula for Step-by-Step method

In the following we will give a general formula for the second order linear differential equation,

$$\begin{aligned} \left(\frac{1}{af}\frac{d^2}{dt^2} + \frac{1}{f}\frac{d}{dt} + 1\right) G_k(t) &= G_{k-1}(t) \\ G_k(0) = 0, \quad \dot{G}_k(0) &= 0 \qquad (k \geq 1) \end{aligned} \tag{87}$$

$$\begin{aligned} \left(\frac{1}{af}\frac{d^2}{dt^2} + \frac{1}{f}\frac{d}{dt} + 1\right) G_0(t) &= G_0(t) \\ G_0(0) = 0, \quad \dot{G}_0(0) &= -a\delta \end{aligned} \tag{88}$$

The solution for the Eq. (88) is

$$G_0(t) = \delta\left(e^{-at} - 1\right) \tag{89}$$

In terms of the function $g_k(\theta)$ defined as follows,

$$G_{k+1}(t) = G_k(t) + \frac{a\delta}{\omega}\left(\frac{af}{\omega^2}\right)^k e^{-\frac{a}{2}t} g_k(\omega t) \qquad (k \geq 0) \tag{90}$$

the initial conditions at $t = 0$ are expressed as

$$\begin{array}{lll} g_k(0) = 0, & g'_k(0) = 0, & (k \geq 1) \\ g_0(0) = 0, & g'_0(0) = 1. & \end{array} \tag{91}$$

From the Eqs. (87), (88) and $\omega^2 = af - a^2/4$, the equation to determine $g_k(\theta)$ is

$$\begin{array}{ll} g''_k(\theta) + g_k(\theta) = g_{k-1}(\theta) & (k \geq 1) \\ g''_0(\theta) + g_0(\theta) = 0 & \end{array} \tag{92}$$

The initial value problem with (91) and (92) may be solved by the functions

$$g_k(\theta) = \frac{1}{2^{2k} k!} \sum_{m=0}^{k} \frac{(2k-m)!}{(k-m)!\, m!} (-1)^{\left[\frac{m+1}{2}\right]} (2\theta)^m \begin{pmatrix} \sin\theta \\ \cos\theta \end{pmatrix}_m \tag{93}$$

Here

$$\begin{pmatrix} \sin\theta \\ \cos\theta \end{pmatrix}_m = \begin{cases} \sin\theta & (m : \text{even}) \\ \cos\theta & (m : \text{odd}) \end{cases} \tag{94}$$

and $[r]$ is the maximum integer which does not exceed r. We give functions for $k = 0, 1, 2, 3$ explicitly.

$$\begin{aligned} g_0(\theta) &= \sin\theta, \\ g_1(\theta) &= \frac{1}{2}\left(\sin\theta - \theta\cos\theta\right), \\ g_2(\theta) &= \frac{1}{8}\Big(3\sin\theta - 3\theta\cos\theta - \theta^2\sin\theta\Big), \\ g_3(\theta) &= \frac{1}{48}\Big(15\sin\theta - 15\theta\cos\theta - 6\theta^2\sin\theta + \theta^3\cos\theta\Big). \end{aligned} \tag{95}$$

In this article, we also use another series of solutions $h_k(t)$ of equations (92) with initial condition;

$$\begin{array}{lll} h_k(0) = 0, & h'_k(0) = 0, & (k \geq 1) \\ h_0(0) = 1, & h'_0(0) = 0. & \end{array} \tag{96}$$

It is easily shown that $h_k(\theta)$ is given by

$$h_k(\theta) = g'_k(\theta) \equiv \frac{\theta}{2k} g_{k-1}(\theta), \tag{97}$$

where the second equality is valid only for $k \geq 1$. We also give $h_k(\theta)$ for $k = 0, 1, 2, 3$ explicitly.

$$\begin{aligned} h_0(\theta) &= \cos\theta, \\ h_1(\theta) &= \frac{1}{2}\theta\sin\theta, \\ h_2(\theta) &= \frac{1}{8}\Big(\theta\sin\theta - \theta^2\cos\theta\Big), \\ h_3(\theta) &= \frac{1}{48}\Big(3\theta\sin\theta - 3\theta^2\cos\theta - \theta^3\sin\theta\Big), \end{aligned} \tag{98}$$

References

[1] M. Bando, K. Hasebe, A. Nakayama, A. Shibata, and Y. Sugiyama, Phys. Rev. **E51** (1995) 1035.

[2] M. Bando, K. Hasebe, A. Nakayama, A. Shibata, and Y. Sugiyama, Japan Journal of Industrial and Applied Mathematics **11** (1994) 203.

[3] M. Bando, K. Hasebe, K. Nakanishi, A. Nakayama, A. Shibata, and Y. Sugiyama, J. Phys. **I** France **5** (1995) 1389.

[4] L. A. Pipes, J. Appl. Phys. **24** (1953) 274.

[5] G. F. Newell, J. Opns. Res. Soc. Am. **9** (1961) 209.

[6] D. C. Gazis, R. Herman and R. W. Rothery, J. Opns. Res. Soc. Am. **9** (1961) 545.

[7] O. Biham, et al., Phys. Rev. **A46** (1992) 6124.

[8] K. Nagel and M. Schreckenberg, J. Phys. **I** France **2** (1992), 2221.

[9] T. Nagatani, J. Phys. Soc. Japan **62** (1993) 3837.

[10] S. Yukawa, M. Kikuchi and S. Tadaki, J. Phys. Soc. Japan **63** (1994) 3609.
S. Yukawa and M. Kikuchi, J. Phys. Soc. Japan **64** (1995) 35.

[11] B. S. Kerner and P. Konhäuser, Phys. Rev. **E48** (1993) 2335.

[12] T. S. Komatsu and S. Sasa, Phys. Rev. E **52** (1995) 5574.

[13] Y. Sugiyama and H. Yamada, DPNU-96-31, June 1996.